# Modeling the Performance of Priority Queueing for Space Communication

Konrad Fuger, Thomas Caffin, Teresa Algarra Ulierte, Andreas Timm-Giel
Hamburg University of Technology (TUHH),
Institute of Communication Networks (ComNets),
Germany
{k.fuger, thomas.caffin.sune.jurgens, teresa.algarra.ulierte, timm-giel}@tuhh.de

***Abstract*—Due to the renewed interest in space exploration in recent years it is expected that the demand for communication services in space will massively increase. As the demand rises, timely and reliable communication becomes a crucial requirement for future missions. Recently traffic prioritization has been demonstrated as a mechanism to improve the quality of service for time-critical data. In this work we propose a mathematical model that describes the delay impact of traffic prioritization on space communication links. Based on a D/M/1 system with two non-preemtive priority classes that captures both retransmission delays over an unreliable channel and queueing delays we derive the full delay distribution for the high priority data. Validated against an extensive simulation campaign across a range of utilizations and priority shares, the model provides an approximation on the Quasi-Realtime probability (the probability of end-to-end delay below 2.5 s), with errors below 5 % at low utilization and up to 38 % at high utilization with a high priority share. For the average delay, the model matches simulation almost exactly across all tested configurations.**

***Index Terms*—Space Communication, Solar System Internet, Queueing Theory, Priority, Quality of Service**

## I. Introduction

The number of planned space missions has been steadily increasing, resulting in a growing demand for communication infrastructures in space [1], [2]. This need for a better infrastructure is currently evolving into a larger framework called the Solar System Internet (SSI), which proposes a similar structure to the terrestial internet on an interplanetary scale [3]. Nevertheless, it has to cater to the conditions of outer space such as large distances, intermittent connectivity, link disruptions, lack of end-to-end path, and large propagation delays [4]. These characteristics require the use of specialized communication architectures such as Delay and Disruption Tolerant Network (DTN), which is well suited for these environments because it employs a store-and-forward transmission mechanism [5]. This approach enables data delivery over intermittent links, even when no end-to-end path exists between source and destination. Furthermore, DTN achieves performance that is equal to or better than that of end-to-end communication mechanisms [6].

Given the constrained infrastructure available in early-stage SSI networks, bottlenecks are a concern in its design [7]. Traffic prioritization has been identified as a solution to mitigate the effects of these bottlenecks by managing increasing communication demands while ensuring adequate Quality of Service (QoS) for time-critical traffic. This is achieved by reducing the delay experienced by high-priority traffic at the expense of potentially increased delays for lower-priority traffic [6], [8]. While previous work has focused on proposing protocol enhancements and evaluating such systems through simulation [6], [8], [9], [10], at the time of writing there is no analytical model describing the impact of traffic prioritization on space communication performance. To address this research gap, this work proposes an analytical model of the delay distribution for a typical space communication link, taking into account different traffic loads and proportions of high- and low-priority traffic.

## II. Related Work

DTNs were initially introduced to address the challenges presented by space communications, and have since been extensively studied. Most of this research has been conducted through simulations, numerical analyses, and in-flight demonstrations [11].

The work presented in [6] simulates a space communication link using a queueing system with two priority classes, equal arrival probabilities, a deterministic arrival process, and a deterministic service process subject to short- and long-term transmission failures. The resulting model provides a realistic representation of a space communication link, as the service process is characterized by the propagation delay caused by the earth-moon distance at the speed of light. Furthermore, the study highlights that short- and long-term transmission failures are important factors to account for, as they model disruptions experienced by communication links over time. Such disruptions may be caused by several phenomena, such as solar flares and unfavourable atmospheric conditions. This mechanism can be evaluated through the use of simulations, as they are relatively simple to implement. However, a drawback of this approach is their time-dependance of the convergence of the simulation results, and thus their reliability. Consequently, analytical modelling can provide insights into the system more quickly and reliably than simulation-based approaches. Such modelling may be an exact formula, an analytical approximation, or a numerical approximation.

The research presented in [12] employs a numerical approximation based on a Non-Gaussian Auto-Regressive model to predict processes from underlying data. A limitation of such models is their reliance on the availability of representative data. Their accuracy may degrade when insufficient data are available, when no relevant data exist, or when the required prediction differs significantly from the available data.

In comparison, analytical approximations can be useful in these scenarios, as they provide insights into system behavior and the influence of different parameters on it. The work presented in [13] describes a complex system through a set of simplifications, enabling a simple analytical model while retaining a high degree of accuracy. The authors further show that the analytical approximation is highly accurate and captures most characteristics of the system behavior. However, large inaccuracies may arise when the underlying assumptions taken for the approximation do not adequately fit the actual system.

Lastly, exact analytical formulas are useful since they provide precise solutions to the problem under consideration. However, deriving such formulas can be complex, and in some cases no closed-form solution may be known. In this regard, the application of prioritization in queueing systems has been widely studied. For example, the work presented in [14] provides a comprehensive treatment of different queueing systems with two non-preemptive priority classes considering a variety of arrival and departure processes. Nevertheless, such approaches have not yet been applied to the specific space communication scenario considered in this work.

## III. Scenario: The Space Communication Link

Space communication channels face a variety of adverse conditions. The vast distances involved result in unavoidable propagation delays ranging from seconds to hours. Moreover, the harsh space environment leads to frequent transmission errors and long-lasting communication outages [7]. To model this behaviour, the channel characterization proposed in previous work is used [6], [7], [8]. Accordingly, a three-state Markov chain is employed to represent a typical earth-to-space communication channel, as depicted in Figure 1.

Whenever the channel is in the **Success** (S) state, transmissions are successful. In contrast, transmissions fail in both the **Short-Term Loss** (ST) and **Long-Term Loss** (LT) states. These two states differ in their temporal characteristics: while the short-term loss state models brief, uncorrelated transmission losses, the long-term loss state represents prolonged link outages caused by natural phenomena such as solar storms. Mathematically, this behavior is realized by choosing $P_{\mathrm{ST-S}} \gg P_{\mathrm{LT-S}}$, causing the system to recover quickly from the short-term loss state while remaining in the long-term loss state for extended periods of time. The complete channel model is characterized by the transition probability matrix $\mathbf{P}$, with states ordered as $(\mathrm{S}, \mathrm{ST}, \mathrm{LT})$.

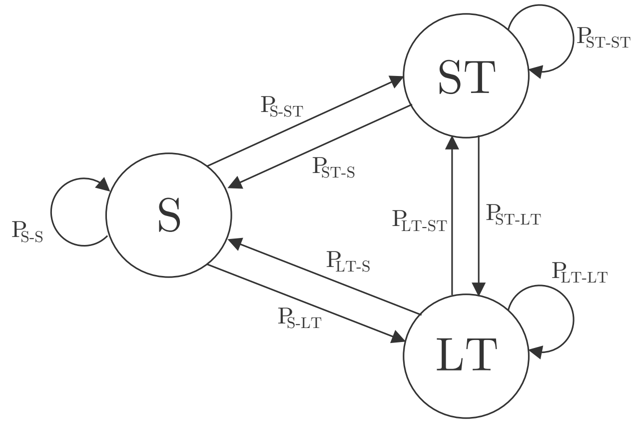


Figure 1: Markov Chain for the channel state [6].

$$\mathbf{P} = \begin{bmatrix} P_{\mathrm{S-S}} & P_{\mathrm{S-ST}} & P_{\mathrm{S-LT}} \\ P_{\mathrm{ST-S}} & P_{\mathrm{ST-ST}} & P_{\mathrm{ST-LT}} \\ P_{\mathrm{LT-S}} & P_{\mathrm{LT-ST}} & P_{\mathrm{LT-LT}} \end{bmatrix}$$

The individual parameters are fitted based on real-world statistics of the occurrence probability of space-weather phenomena [6] and the time between state transitions of the channel is set to $\Delta t = 1\,\mathrm{s}$.

Further, a simple Stop-and-Wait Automatic Repeat Request (ARQ) is considered to realize the custody transfer stipulated by the Bundle Protocol [15] commonly used in space communication. Here, failed transmissions (i.e. when the channel is in the short-term loss or long-term loss states) are detected when no acknowledgement is received after one round-trip-time. In this case, the bundle is retransmitted until the channel transitions back to the success state. Because of the vast distances in space, the round-trip-time is approximated by twice the propagation delay $d_{\mathrm{prop}}$ between earth and moon (roughly 1.28 s). For the sake of simplicity, we assume the previous transmission has just succeeded and the Markov chain transitions into a new state[1]. Using the law of total probability, we can calculate the probability that exactly $n$ transmissions are needed based on the channel state $C$ at the beginning of the first transmission attempt:

$$\Pr\{\text{need } n \text{ tx}\} = \sum_{i \in \mathcal{C}} \Pr\{\text{need } n \text{ tx} \mid C = i\} \cdot \mathbf{P}_{\mathrm{S},i}. \quad (1)$$

where $\mathbf{P}_{\mathrm{S},i}$ denotes the probability to move from the success state into a given state $i$ in a single transition of the Markov chain. The conditional probabilities are directly obtained from the transition matrix $\mathbf{P}$. For this, we evaluate the channel at the possible transmission arrival times $d_{\mathrm{prop}}$, $3d_{\mathrm{prop}}$, $5d_{\mathrm{prop}}$ etc. For the $n$-th transmission, the corresponding number of Markov chain transitions is $m_n$:

[1]In reality, the transmission times and changes of the channel state are not synchronized, but our investigation shows no major penalty from this simplification.

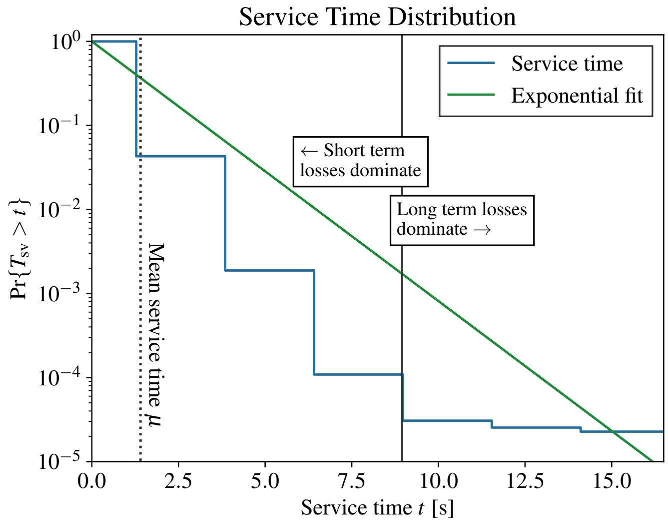


Figure 2: Service time distribution for the space communication link with exponential fit

$$m_n = \left\lfloor \frac{(2n-1)d_{\text{prop}}}{\Delta t} \right\rfloor . \tag{2}$$

Only transitions into the success state matter at these times. Abbreviating $p_{i,n} = \Pr\{\text{need } n \text{ tx} \mid C = i\}$, the conditional probabilities are accumulated recursively as

$$p_{i,n} = \left(1 - \sum_{k=1}^{n-1} p_{i,k}\right) \cdot (\mathbf{P}^{m_n})_{i,\mathrm{S}}, \quad n \geq 1, \tag{3}$$

where the empty sum for $n = 1$ evaluates to zero. Since every failed attempt adds one round-trip-time, the service time distribution $f_S(t)$ is expressed as a series of Dirac-impulses at the possible arrival times weighted with the corresponding probabilities.

$$f_S(t) = \sum_{n=1}^{\infty} \delta(t - (2n-1) \cdot d_{\text{prop}}) \cdot \Pr\{\text{need } n \text{ tx}\}. \tag{4}$$

The service time distribution is shown in Figure 2. As expected, the service time generally exhibits a staircase pattern with a geometric decay representing the successive retransmission attempts. Additionally, we can clearly identify the difference between short term and long term losses. Service times up to ca. 9 s are predominantly caused by short-term losses and longer service times are caused by long-term losses represented by a more shallow geometric decay. While the above derivation yields an exact mathematical description of the service time distribution, for the purpose of modelling queueing in such a system, we chose to approximate the service time with an exponential fit (green line) matched to the analytically derived effective service rate $\mu$.

$$\mu = \left[\int_{t=0}^{\infty} f_S(t) \cdot t \,\mathrm{d}t\right]^{-1} \tag{5}$$

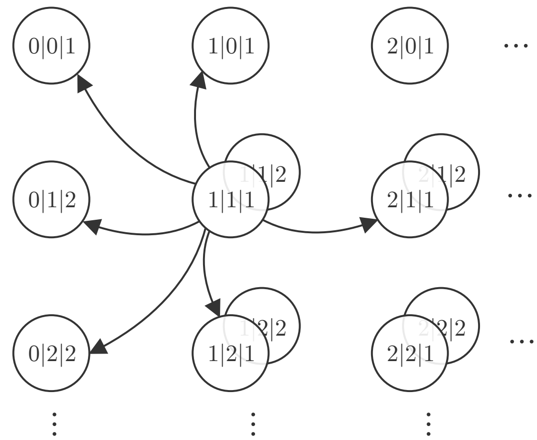


Figure 3: Embedded Markov chain representing the queue state at arrival instances with exemplary transitions out of the $(1\,|\,1\,|\,1)$ state.

This simplification produces two significant modelling artifacts: First, the exponential fit incorrectly predicts the possibility that packets are delivered faster than the propagation delay, which we will address in the further derivation of the model. Second, as our exponential fit needs to incorporate both long- and short-term losses, it overestimates the delay while short-term losses are dominant and underestimates it when long-term losses are dominant. Nevertheless, the exponential fit captures the general shape of the service time distribution.

## IV. Modelling of Priority Queues

Using the above simplification to treat the departure process as a Poisson process, allows us to classify the resulting queueing system as a D/M/1 system with two non-preemtive priorities. Matching prior investigations [6], the bundles of both priorities arrive with a deterministic arrival rate $\lambda$ and the probability of an arriving bundle being of high priority is denoted with $q_h$, while the probability of a low priority bundle arriving is $q_\ell = 1 - q_h$. We represent the state of the queueing system at arrival instances with the embedded Markov chain displayed in Figure 3.

In doing so, we follow the approach of [14] to use three random variables to describe the state of the queueing system at any arrival instance $n$:

- $X_n \in \mathbb{N}_0$ indicates the number of **high priority** bundles in the system at arrival instance $n$,
- $Y_n \in \mathbb{N}_0$ describes the number of **low priority** bundles in the system and
- $Z_n \in \{1, 2\}$ accounts for the type of bundle currently in service, where $Z_n = 2$ means a low priority bundle is currently being served and $Z_n = 1$ indicates service of a high priority bundle or the system being empty.

These random variables form a three-dimensional state space $S_{\mathrm{Q}} = \{X, Y, Z\}$ with steady-state probabilities $\pi_{ijk}$. Since we model the system at arrival instances, we can identify the transition probabilities by calculating the probability to have a certain number $k$ of departures during a single inter-arrival time:

$$a_k = \int_0^\infty \frac{(\mu t)^k}{k!} e^{-\mu t} f_A(t)\,\mathrm{d}t = \frac{(1/\rho)^k}{k!} e^{-1/\rho} \tag{6}$$

Since the arrival time distribution $f_A(t)$ is deterministic, this results in a Poisson distribution with mean $1/\rho$, with $\rho = \lambda/\mu$ being the system utilization. For example, the probability to move from state $(1\,|\,1\,|\,1)$ to $(2\,|\,1\,|\,1)$ equals $a_0 \cdot q_h$ as this state transition only happens if no service completes during one arrival time and the arriving bundle is of high priority. A transition from $(1\,|\,1\,|\,2)$ to $(1\,|\,1\,|\,1)$ requires that the low priority bundle currently in service completes and that the arriving bundle is again of low priority (Probability $a_1 \cdot q_\ell$). Following the same procedure, all transition probabilities are identified accounting for the number of bundles in the system and the priority class currently in service. A comprehensive derivation is provided in [14]. To calculate the steady-state distribution of the queueing system, a set of generating functions is introduced

$$\begin{aligned}\Gamma(y,z) &= \sum_{i=0}^{\infty}\sum_{j=1}^{\infty} \pi_{ij2} \cdot z^j y^i \\ \Pi(y,z) &= \sum_{i=0}^{\infty}\sum_{j=0}^{\infty} \pi_{ij1} \cdot z^j y^i\end{aligned} \tag{7}$$

where the $y$ variables is conjugate to the number of high priority bundles and the $z$ variable to the number of low priority bundles. Using the transition probabilities identified by inspection of the embedded Markov chain, a closed-form generating function for the number of high priority bundles when $Z = 2$ is found to be

$$\Gamma(y,1) = \frac{q_h a_o (\eta - \gamma)}{\left(1 - a_0\left(q_h y + q_\ell\right)\right)\gamma}. \tag{8}$$

The generating function for the number of high-priority bundles when $Z = 1$ equals

$$\Pi(y,1) = \frac{1-\eta}{1-\gamma y} - \frac{y\left(q_h a_0 - (1 - a_0 q_\ell)\,\gamma\right)\Gamma(y,1)}{q_h a_0\left(1 - \gamma y\right)}, \tag{9}$$

where $\eta$ and $\gamma$ are obtained from the equations:

$$\eta = \bar{f}_A(\mu - \mu\eta) \ \text{ and } \ \gamma = (q_h + q_\ell\gamma)\bar{f}_A(\mu - \mu\gamma). \tag{10}$$

with $\bar{f}_A(s)$ being the Laplace transform of the inter-arrival time distribution. Again, a full derivation can be found in [14]. This finally allows for the extraction the probabilities to have $i$ high priority bundles in the system $\pi_i^h$ by repeated differentiation and evaluation at $y = 0$:

$$\pi_i^h = \frac{1}{i!}\left.\frac{d^i\big(\Pi(y,1) + \Gamma(y,1)\big)}{dy^i}\right|_{y=0} \tag{11}$$

While the steady-state distribution is an important result, our final goal is the derivation of the end-to-end delay distribution. For this purpose, we first derive the waiting time of a high priority bundle considering three mutually exclusive and collectively exhaustive cases:

- $A_0$: The system is empty,
- $A_i,\ i \geq 1$: There are $i$ high priority bundles in the system, one of them bing served,
- $B_i$: There are $i$ high priority bundles in the system, but a low priority bundle is currently being served.

Since there is no waiting time when the system is empty, we can express the Laplace transform of the waiting time of a high priority bundle as $\bar{w}_h(s)$.

$$\begin{aligned}\bar{w}_h(s) = &\sum_{i=0}^{\infty}\left(\frac{\mu}{\mu+s}\right)^i \cdot \Pr\{A_i\} \\ &+ \sum_{i=0}^{\infty}\left(\frac{\mu}{\mu+s}\right)^{i+1} \cdot \Pr\{B_i\}\end{aligned} \tag{12}$$

which we can simplify using the generating functions introduced earlier.

$$\bar{w}_h(s) = \Pi\left(\frac{\mu}{\mu+s}, 1\right) + \frac{\mu}{\mu+s}\Gamma\left(\frac{\mu}{\mu+s}, 1\right) \tag{13}$$

Finally, this yields a closed form solution of $\bar{w}_h(s)$

$$\bar{w}_h(s) = \frac{(\mu+s)(1-\eta)}{\mu+s-\gamma\mu} + \frac{\mu(\eta-\gamma)}{\mu+s-\gamma\mu} \tag{14}$$

To get the delay of the high priority bundles, we need to add one more service time. Even though up to this point we have used the simplified exponential service time distribution, here we deviate from this and use the accurate description obtained in Section III which yields a complete model for the end-to-end delay.

$$\bar{d}_h(s) = \bar{w}_h(s) \cdot \bar{f}_S(s) \tag{15}$$

Using the accurate service time distribution also rectifies the modelling artifacts discussed earlier which would allow end-to-end delays lower than the propagation delay.

## V. Results

The derived model is evaluated by simulating the space communication link scenario for various combinations of utilization $\rho$ and high priority share $q_h$ (while $q_h + q_\ell = 1$). Each simulation is repeated 40 times and the end-to-end delay including queueing and service is recorded for each bundle in the simulation together with its priority class. The delay distribution for an exemplary utilization of $\rho = 0.8$ and a priority share of $q_h = 0.25$ is shown in Figure 4. The simulation results (solid lines) show the expected result of an

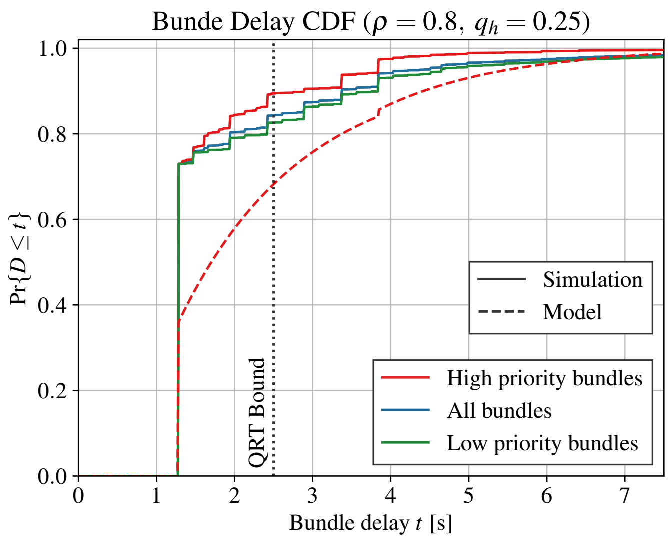


Figure 4: End-to-end bundle delay distribution

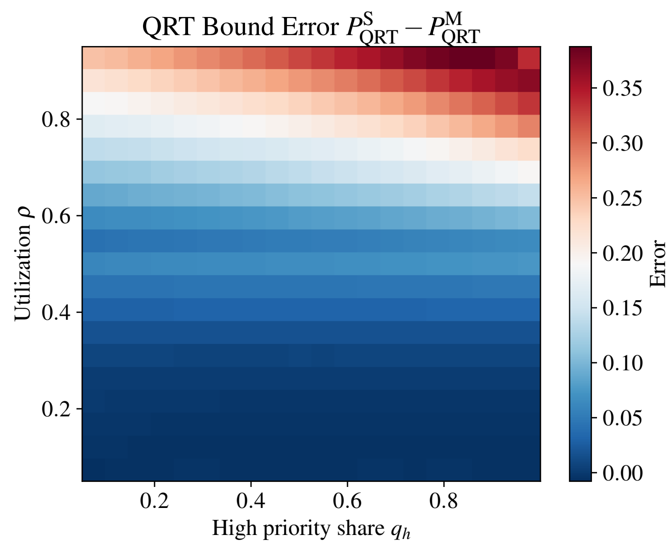


Figure 5: QRT probability error for various utilizations and priority shares

improved performance of high priority bundles (red) at the expense of low priority bundles (green). As only a quarter of the generated bundles are of high priority, the penalty for low priority bundles is small yielding a performance comparable to a system without priorities (blue). Additionally, Figure 4 shows the modelled delay CDF for high priority bundles as a dashed line. While the model correctly predicts that the delay has to be at least one propagation delay $d_{\text{prop}}$ and that delays of more than 6 s are extremely unlikely, it also shows deviations from the simulation results. As we approximate the service process as a Poisson process, the model generally predicts longer queues and therefore higher delays. This results in the model serving as a lower bound for the achievable performance, especially when the Quasi-Realtime (QRT) probability is concerned, which is the probability that the delay is less than 2.5 s.

We can obtain deeper insights into this when evaluating the QRT probability over all combinations of utilization and priority share. Figure 5 shows the error in QRT probability between model and simulation. From this we can clearly see that the error is either negligible or positive, indicating that the model is effective in predicting a lower bound of the QRT probability. Especially for low utilization, we observe very low errors, as the delay (and with that the QRT probability) is dominated by the service time which is modelled without any simplifications. Only for high utilization, where queueing becomes a significant effect, the error rises. For low values of the high priority share $q_h$ we see a modest increase as the queues consist predominantly of low priority bundles that are skipped over. Only for high utilization and a high priority share, the error rises to as much as 38 %.

While the QRT probability is the most important KPI from an application perspective, the model provides further insights. For example, we can use the derived delay distribution to calculate the average delay for both priority classes. For this we leverage the fact that the system is work-conservative and therefore the prioritization only shifts delay from one class to another. Therefore, we can express the average delay $\mathbb{E}[D]$ of a random bundle as a combination of the average delay of the individual priority classes ($D_l$ and $D_h$):

$$\mathbb{E}[D] = q_h \cdot \mathbb{E}[D_h] + q_\ell \cdot \mathbb{E}[D_l] \tag{16}$$

where $\mathbb{E}[D]$ is derived with the well-known expression for a classical D/M/1 system (a special case our model incorporates when $q_h = 1$).

The results are shown in Figure 6 again using an exemplary utilization of $\rho = 0.8$ with varying values of $q_h$. As expected, the average delay of a random bundle (blue) is unaffected by shifting priority shares. It is also well described by the modelling results. For a low value of the high priority share $q_h = 0.1$ the delay of an average bundle also closely aligns with the delay of a low priority bundle (green) as most bundles are in fact low priority bundles and the probability of a high priority bundle arriving, that would skip in front of the lower priority, is low. In this configuration we also see the highest gain for high priority bundles reducing their average delay by more than 40 % compared to an average bundle. Only when we increase $q_h$, the gap closes and the high priority performance resembles the performance of an average bundle more closely. In doing so the average delay for low priority bundles quickly deteriorates. The model describes these effects with a high accuracy again exhibiting negligible errors for the high priority and slightly underestimating the delay for high low priority bundles.

Finally, the model can be used to predict the queue lengths of the space communication link, which is an important result for dimensioning space communication hardware. While the generating functions introduced in Section IV can be used to produce the distribution of queue lengths for the high priority class and therefore also describe the probability of a

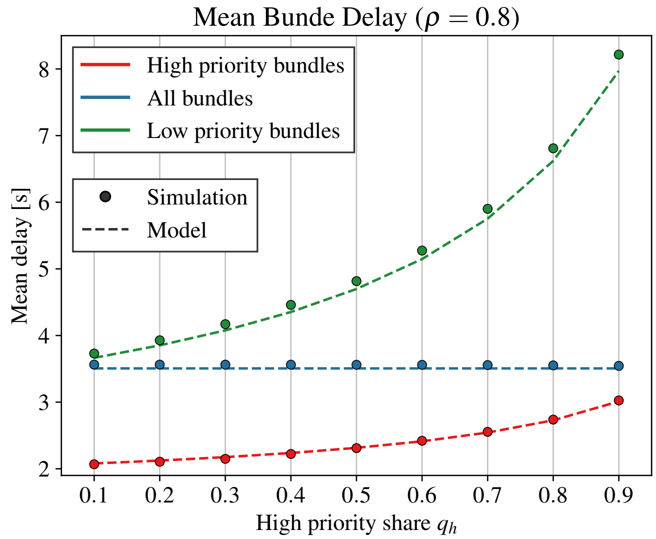


Figure 6: Mean delay for different priority classes over various priority shares

fixed-size queue overflowing, we can utilize Littles law to get the average queue lengths for both classes using the average delay obtained above:

$$\begin{aligned} L &= L_h + L_\ell \\ \lambda\,\mathbb{E}[D] &= q_h \cdot \lambda\,\mathbb{E}[D_h] + q_\ell \cdot \lambda\,\mathbb{E}[D_l] \end{aligned} \tag{17}$$

with $L_h$ and $L_\ell$ being the average queue length of the low and high priority bundles respectively. This result shows that the queue lengths are proportional to the average delay presented in Figure 6 as well as the priority shares $q_h$ and $q_\ell$ which allows for an initial dimensioning of both priority queues.

## VI. Conclusion & Future Work

Prioritization in space communication systems is a critical mechanism to realize the future Solar System Internet. In addition to the development of protocols that incorporate prioritization into Bundle Protocol [17], [18], the theoretical understanding and modelling of the achievable performance plays a crucial role. To this end, this paper proposes a queueing-theory based model of the delay distributions for space communication links. It does so by analyzing the service times achieved over a typical space communication link before applying a two-priority D/M/1 queueing system to derive the delay distributions. Comparing the obtained results with simulation results we find that the model provides a good approximation of the QRT probability, one of the most important KPIs in space communication. Further, we apply the model to predict average delays where the model shows an excellent fit and accurately describes the impact of a varying priority share.

Building on top of the presented results future work will extend the derived delay distributions from single links to multi-hop paths. As the performance of these, like the performance of the individual links, depends on the link utilization as well as the priority share, modelling the end-to-end performance subsequently offers an opportunity to optimize routing of the traffic based on the available paths.

## References


[1] M Cosby et al., "The future lunar communications architecture," *Washington, DC USA: the Interagency Operations Advisory Group (Lunar Communications Architecture Working Group)*, 2022.

[2] Interagency Operations Advisory Group, "The Future Lunar Communications Architecture," 2022. Accessed: Oct. 14, 2024. [Online]. Available: https://www.ioag.org/Public%20Documents/Lunar%20communications%20architecture%20study%20report%20FINAL%20v1.3.pdf.

[3] I. C. Internet Society, *Solar system internet: Architecture and governance*, 2024. Accessed: Sep. 12, 2025. [Online]. Available: https://drive.google.com/file/d/1anMcVEqXjNtk5gdo_qce28SowusXKkfi/view.

[4] F. Warthman, *Delay-and disruption-tolerant networks (dtns)*. Accessed: Sep. 12, 2025. [Online]. Available: https://www.nasa.gov/wp-content/uploads/2023/09/dtn-tutorial-v3.2-0.pdf.

[5] L. Torgerson et al., *Delay-tolerant networking architecture*, RFC 4838, 2007.

[6] T. Algarra Ulierte, K. Kuladinithi, A. Timm-Giel, and F. Flentge, "Lunar communication services: Feasibility study on traffic prioritization of quasi-real time communications over dtns," in *2023 IEEE International Conference on Wireless for Space and Extreme Environments (WiSEE)*, 2023, pp. 35–40.

[7] T. Algarra Ulierte, F. Flentge, J. Quintanilla, and A. Timm-Giel, "Characterizing space communication channel behaviour: An analytical approach with esa mission data validation," in *10th International Workshop on Tracking, Telemetry and Command Systems for Space Applications (TTC)*, IEEE, 2025.

[8] T. Algarra Ulierte, K. Kuladinithi, A. Timm-Giel, and F. Flentge, "Enabling traffic prioritization for space communications over dtns," *IEEE Journal of Radio Frequency Identification*, vol. 8, pp. 748–760, 2024.

[9] T. Algarra Ulierte, K. Kuladinithi, A. Timm-Giel, and F. Flentge, "Adding Quality of Service Support to Bundle Protocol Through an Extension Block," *IEEE International Conference on Space Mission Challenges for Information Technology and Space Computing Conference*, 2024.

[10] T. Algarra Ulierte, F. Flentge, and A. Timm-Giel, "Quality of service extension for delay- and disruption-tolerant networking," in *18th International Conference on Space Operations (SpaceOps)*, 2025.

[11] C. Malnati and F. Flentge, "Dtn demonstrations with esa ground segment," *IEEE Journal of Radio Frequency Identification*, vol. 8, pp. 609–617, 2024.

[12] T. J. Hu, X. X. Huang, and Q. Tan, "Time delay prediction for space teleoperation based on non-gaussian auto-regressive model," in *2012 Proceedings of International Conference on Modelling, Identification and Control*, 2012, pp. 567–572.

[13] X. Jin and G. Min, "Modelling and analysis of priority queueing systems with multi-class self-similar network traffic: A novel and efficient queue-decomposition approach," *IEEE Transactions on Communications*, vol. 57, no. 5, pp. 1444–1452, 2009.

[14] R. Reed, "Priority queues," Ph.D. dissertation, Durham University, 1971.

[15] K. Scott and S. Burleigh, "Bundle protocol specification," Tech. Rep., 2007.

[16] O. Tange, *Gnu parallel 20251022 ('goodall')*, Oct. 2025. [Online]. Available: https://doi.org/10.5281/zenodo.17488917.

[17] T. Algarra Ulierte, K. Kuladinithi, A. Timm-Giel, and F. Flentge, "Enabling traffic prioritization for space communications over dtns," *IEEE Journal of Radio Frequency Identification*, vol. 8, pp. 748–760, 2024.

[18] T. Algarra Ulierte, K. Kuladinithi, A. Timm-Giel, and F. Flentge, "Adding quality of service support to bundle protocol through an extension block," in *2024 IEEE 10th International Conference on Space Mission Challenges for Information Technology (SMC-IT)*, 2024, pp. 115–124.